Influence of sintering temperature on the development of alumina membrane shaped by centrifugal casting for gas separation

R. C. T. Bertotto[1]*, M. Virginie[2], A. Khodakov[2], A. Ambrosi[1], L. D. Pollo[1], N. R. Marcilio[3], I. C. Tessaro[1]
[1]Universidade Federal do Rio Grande do Sul, Departamento de Engenharia Química, Laboratory of Packaging Technology and Membrane Development, R. Ramiro Barcelos 2777, Porto Alegre, RS, Brazil
[2]Université Lille 1, Sciences & Technologies, Unité de Catalyse et Chimie du Solide, UMR 8181 CNRS, France
[3]Universidade Federal do Rio Grande do Sul, Departamento de Engenharia Química, Laboratory of Waste Processing, Porto Alegre, RS, Brazil

Abstract

The development of ceramic membranes for the most diverse separation processes has gained high visibility, mainly due to their better performance in harsh environments in comparison to polymeric materials. Among the different techniques used to prepare tubular ceramic membranes, the centrifugal casting (CC) is interesting for obtaining highly homogeneous structures, essential for gas separations. This study assessed the influence of two sintering temperatures (1450 and 1500 °C) of alumina membranes prepared by CC on the membrane morphology and on the permeation of helium, nitrogen and oxygen gases. The membranes were characterized by their morphology, apparent porosity, and gas permeation. The results indicated that the sintering temperature is a fundamental parameter for controlling membrane properties, an increase of only 50 °C led to a tenfold decrease in the gas permeate flux, indicating densification of membrane porous structure. This was in accordance with the results observed in the membrane micrographs and the apparent porosity.
Keywords: centrifugal casting, gas separation, ceramic membrane.

INTRODUCTION

Gas separation processes are present in several industrial areas. The hydrogen recovery in petroleum refining, the separation of nitrogen and oxygen from air, and the separation and recovery of carbon dioxide from biogas and syngas are examples of operations that have gained attention in relation to the use of membranes to promote the separation [1, 2]. In these processes, the membrane acts as a selective barrier, allowing or restricting components to pass based on the affinity of the molecules with the membrane material or on the difference of sizes between membrane pores and the molecules [3]. In this sense, membranes can be manufactured from different organic and inorganic materials to have a required characteristic for a given separation. Inorganic membranes had received fairly little attention for gas separation until the late 1990s. This has mainly been due to their porous structure and therefore less ability to separate gas molecules [4]. However, the use of inorganic membranes presents some advantages due to their extremely high thermal, chemical, mechanical and physical stability. Ceramic membranes are useful to withstand extreme conditions of gas operations such as large pH ranges, high temperatures, and high operating pressures without compaction and swelling, issues that commonly affect polymeric membranes. These characteristics make them applicable in several situations where polymeric membranes are not suitable to be used [5, 6].

Aluminum oxide or alumina (Al_2O_3) is one of the most used oxides for the production of inorganic (ceramic) membranes because of its great properties and high availability [2]. Among the techniques for preparing ceramic membranes are the extrusion, a widely studied and widespread method [7-10], the isostatic pressing, and the centrifugal casting [11, 12], a technique typically used to cast thin-walled metallic cylinders, where a molten metal is centrifugally thrown against the inner wall of a cylindrical mold at a high speed, and solidifies after cooling. The centrifugal casting produces ceramic membranes structures with distinct properties when compared to the other techniques. The main advantage is the uniformity in particle packing, which results in a very homogeneous product with higher strength and a smoother inner surface [13, 14]. In this process, the powder is dispersed in a liquid to obtain a ceramic slurry, which is poured inside the cylindrical mold that rotates around its own central axis. The ceramic tube formed must be properly released and treated to result in a compact and homogeneous tubular structure [13, 15]. After drying, the green ceramic tube is sintered at elevated temperatures to increase its mechanical strength. Morphological characteristics of the tube such as pore shape, surface area and porosity, and the neck area and grain size of alumina are modified during the sintering process [16-18],

**renata.teles@ufrgs.br*
https://orcid.org/0000-0002-6589-9745

impacting the performance of the selective layer to separate gas molecules. The sintering procedure should be carefully designed to strengthen the structure without totally densify the green tube, but little attention has been given to this step in relation to the membranes prepared by the centrifugal casting method. Thus, the present study focused on preparing tubular alumina-based ceramic membranes using the centrifugal casting technique and evaluating the effects of two different sintering temperatures on the tube's properties. The tubes were characterized according to the morphology, the porosity and the permeation performance to pure gases.

MATERIALS AND METHODS

Raw material: the alumina powder (CT3000SG, Almatis, 99% Al_2O_3) was used for the centrifugal fabrication of ceramic tubes. Table I shows the main properties of the powder used, as supplied by the manufacturer. Distilled water was used to prepare the slurry and no dispersing agent was used.

Table I - Properties of the CT300SG alumina powder.

Property/method	Typical	Min	Max
Specific surface area/BET (m^2/g)	7.5	6.5	8.5
Particle size/D50 Cilas (μm)	0.5	0.3	0.6
Chemical analysis (%)			
Na_2O	0.08		0.10
Fe_2O_3	0.02		0.03
SiO_2	0.03		0.07
CaO	0.02		0.03
MgO	0.07	0.05	0.10

Membrane preparation: the aqueous ceramic slurry was prepared by mixing 40 wt% alumina and 60 wt% distilled water. The slurry was kept under stirring at room temperature (~25 °C) for 20 min and subsequently sonicated for 10 min for removing air bubbles incorporated into the slurry during the stirring step. The slurry was poured into stainless steel tubes (length of 170 mm and internal diameter of 10 mm) with lids on both sides. The molds were placed in a special equipment (Fig. 1) and rotated at 4000 rpm for 8 min. The green ceramic tubes were dried at room temperature (~25 °C) for 48 h and then removed from the molds. Sintering was performed in a bench scale furnace (P330, Nabertherm) using the following ramp conditions: i) heating rate of 1 °C/min from room temperature to 100 °C; ii) step at 100 °C for 60 min; iii) heating rate of 5 °C/min to 1100 °C; iv) step at 1100 °C for 60 min; v) heating rate of 5 °C/min to the last temperature (1450 or 1500 °C); and vi) step for 180 min.

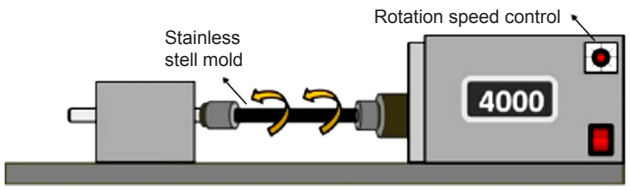

Figure 1: Scheme of the system used in the preparation of ceramic tubular membranes.

Alumina characterization: the phase identification of the commercial alumina CT3000SG was evaluated by X-ray diffraction (XRD, X'Pert MDP, Phillips; X-ray tube with CuKα radiation).

Membranes characterization: the morphology of the external and inner surfaces and the cross-section of the ceramic membrane was analyzed by scanning electron microscopy (SEM, JSM 6060, Jeol; 15 kV, with gold plating). The apparent porosity of the ceramic membrane was determined by the Archimedes method (immersion) using distilled water, based on ISO 10545-3. This method can be used as an estimative of the membrane porosity, as suggested in [19-22]. Gas permeation tests were performed in a bench scale permeation unit (Fig. 2) with pure gases (helium, nitrogen, and oxygen). The tubular ceramic membrane was sealed and placed in a custom-made permeation module. The gas flow rate measurements were performed at room temperature (~25 °C) with a variable transmembrane pressure difference from 1 to 5 bar. The volumetric flow rates were determined by a variable volume method using a soap bubble flowmeter. The permeance of each gas was then calculated by:

$$\frac{Pi}{1} = \frac{Q_i}{A.\Delta P} \qquad (A)$$

where Q_i is the volumetric flow rate of gas i in the standard temperature and pressure, l is the thickness of the membrane (cm), A is the effective membrane area (cm^2) and ΔP is the transmembrane pressure difference (cmHg). This equation is usually expressed in gas permeation unit [GPU=10^{-6}.cm^3(CNTP).cm^{-2}.s^{-1}.$cmHg^{-1}$]. The membrane selectivity ($\alpha_{i/j}$) was evaluated in terms of ideal selectivity, calculated from the ratio of the pure gas permeances:

$$\alpha_{i/j} = \frac{P_i}{P_j} \qquad (B)$$

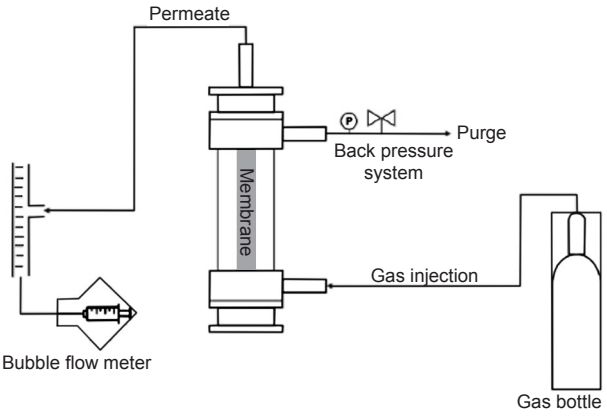

Figure 2: Scheme of gas permeation setup.

RESULTS AND DISCUSSION

Alumina characterization: the XRD pattern used to identify the phases of the alumina powder is presented in Fig. 3. Due to the characteristic peaks identified in the diffractogram in the scanning region from 10° to 70° (25°, 35°, 37°, 43°, 52°, 57°, 59°, 61°, 66°, and 68°), it may be inferred that the commercial alumina CT3000SG was composed essentially by the crystalline phase alpha (α) alumina. Contreras et al. [23] and Martín-Ruiz et al. [24] found peaks with the same values of angles when characterizing alumina that also presented the crystalline phase of the type α. The alpha phase of alumina is considered one of the most stable and with great possibilities for applications, due to its good mechanical, thermal and electrical properties [25].

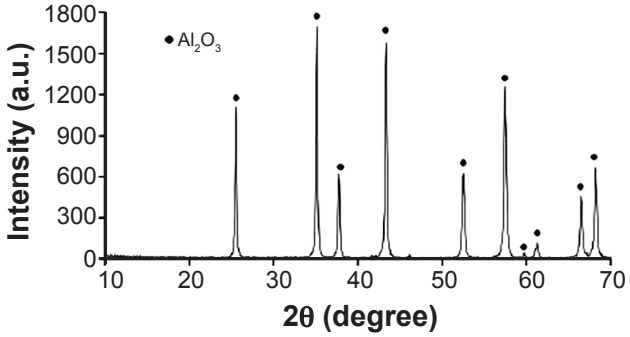

Figure 3: XRD pattern of CT3000SG powder.

Membrane characterization: the morphology of the external and inner surfaces and the cross-section of the ceramic membranes sintered at 1450 and 1500 °C are shown in Fig. 4. Comparing the SEM images of the external surface with the images of the inner surface it was possible to verify that the later were smoother and more uniform than the former. The irregularities present outside the membrane were probably generated by the direct contact between the ceramic tube formed and the stainless-steel mold. The better homogeneity of the inner surface may indicate that smaller particles, with lower mass, were deposited over larger particles or that the particles were better organized in the tube structure. This could be a consequence of the centrifugal force, which pushed the heavier particles to outside of the tube center more easily than the lighter particles, as already observed in [16, 26-29], but analyzing the cross-section images, it was possible to note that the membrane morphology was practically symmetric for both sintering temperatures, 1450 and 1500 °C. This meant that the rotation speed used in this work promoted a homogeneous dispersion of the alumina particles in the structure, obtaining symmetric pore size distribution and good densification of membrane structure [30]. It was also possible to verify that the increase of sintering temperature resulted in a more densified structure, which was in accordance to the effects produced by higher temperatures, once the grain growth affects the structural characteristics like porosity and density of ceramic tube [26, 31]. The apparent porosity, measured by the Archimedes method, was performed to complement the results obtained in SEM analysis. The values obtained were 7% and 2.6% for the tubes sintered at 1450 and 1500 ºC, respectively. As expected, the membrane porosity decreased when the sintering temperature increased. The decrease in porosity and an increase of densification with increased sintering temperature confirmed the results from SEM analysis of cross-sections and by others [16, 26].

The gas separation performance of the ceramic membranes was assessed through gas permeation tests, employing pure helium (He), nitrogen (N_2) and oxygen (O_2). The permeances of each gas are reported in Fig. 5. The results obtained in the permeation tests evidenced the direct relation between the sintering temperature and the gas permeances. The gas fluxes increased when the feed pressure was increased, which was in accordance with the theory [32]. When comparing the different sintering temperatures, it was possible to observe that the increase of only 50 ºC resulted in a tenfold reduction of the gas permeances. For the membrane sintered at 1450 °C, it was not possible to measure the He permeation when the pressure was higher

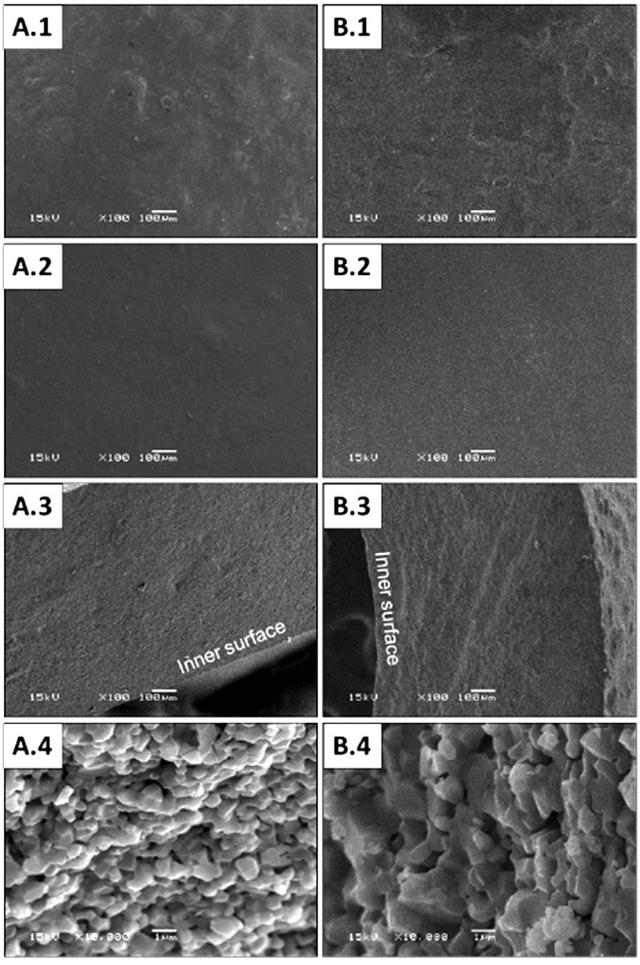

Figure 4: SEM micrographs of surface and cross section of ceramic membranes sintered at: A) 1450 °C; and B) 1500 °C. 1-external surface, 2-inner surface, 3-cross-section, and 4-zoom of cross-section.

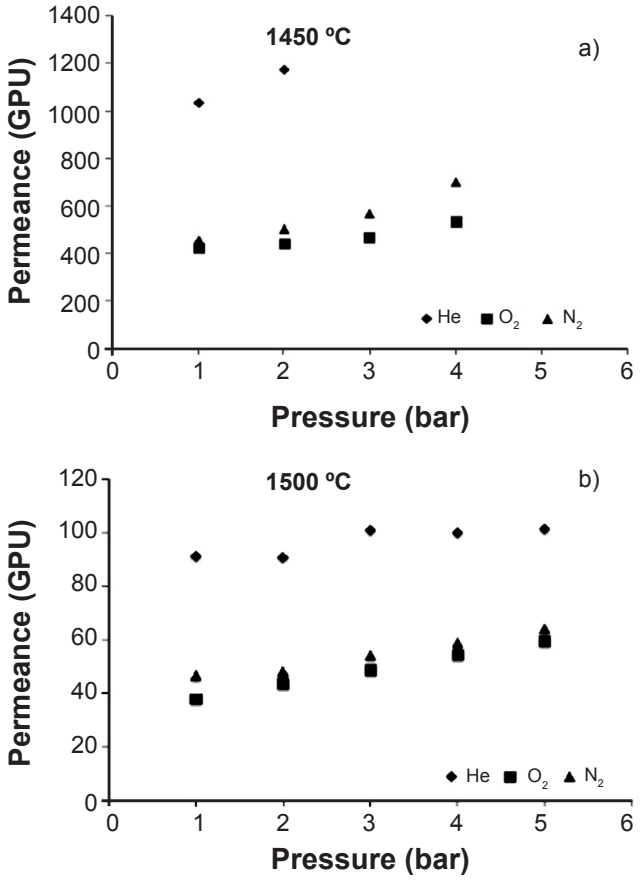

Figure 5: Gas permeance obtained in the pure gas permeation tests for the centrifugal casting ceramic membranes. a) 1450 ºC; and b) 1500 ºC.

than 2 bar, and the N_2 and O_2 permeation when the pressure was higher than 4 bar. On the other hand, it was possible to perform the tests in the full range of pressures and flow rates of the equipment for the membrane produced at 1500 °C. The results were directly related to the effects of the temperature on the sintering of alumina, once higher temperatures densified the structure [11], reinforcing the results obtained in the porosity measurements and on a certain extent the SEM analysis.

The ideal selectivities to each specific pressure tested are presented in Table II for He/N_2, He/O_2 and O_2/N_2 pairs of gases. The ideal selectivity obtained could be compared to the Knudsen selectivity, which was calculated from the square root of the inverse molecular weight of the two gases (He/O_2=3.0, He/N_2=2.6, O_2/N_2=0.9) [3]. The selectivities of the membrane sintered at 1450 °C were close to the Knudsen selectivity for all pairs of gases, mainly at 2 bar. For the membranes sintered at 1500 °C, only the pair O_2/N_2 presented values comparable to the ideal Knudsen selectivity. These results indicated parallel transport mechanisms, such as surface diffusion and Knudsen diffusion. The mechanisms may have occurred simultaneously due to the differences of pores size and their distribution on the membrane surface, which may have affected the affinity of the membrane with the gas molecules transported [5]. Evaluating the influence of pressure on the ideal selectivity results for the different pairs of gases, in general, the increase in pressure reduced the ideal selectivity values. Similar results were reported in the literature, since an increase in system pressure, the driving force of the process, increases the gas permeance and reduces the ideal selectivity [33, 34].

Table II - Ideal selectivities obtained in the pure gas permeation tests for the ceramic membranes.

Pressure (bar)	1450 °C			1500 °C		
	He/O_2	He/N_2	O_2/N_2	He/O_2	He/N_2	O_2/N_2
1	2.4	2.3	0.9	2.4	1.9	0.8
2	2.7	2.3	0.9	2.1	1.9	0.9
3	-	-	0.8	2.1	1.9	0.9
4	-	-	0.8	1.8	1.7	0.9
5	-	-	-	1.7	1.6	0.9

CONCLUSIONS

The present study evaluated the effects of the sintering temperature on α-alumina gas separation membranes prepared by the centrifugal casting technique. The ceramic tubes obtained were characterized by SEM, apparent porosity and gas permeation (He, N_2, O_2). The higher sintering temperature reduced the apparent porosity and the permeance of gases, but had a minor effect on the ideal selectivity. Gases permeances followed the order $He>N_2\approx O_2$, and the ideal selectivities indicated parallel transport mechanisms. The ceramic membranes developed have the potential for being applied in gas separation processes, but the preparation methodology must be improved for increasing their selectivity while keeping their gas permeances.

ACKNOWLEDGMENTS

Authors thank the financial support of Coordenação de Aperfeiçoamento de Pessoal de Nível Superior (CAPES), Conselho Nacional de Desenvolvimento Científico e Tecnológico (CNPQ), Fundação de Amparo à Pesquisa do Estado do RS (FAPERGS) and Almatis for supplying raw ceramic powder.

REFERENCES

[1] P. Li, Z. Wang, Z. Qiao, Y. Liu, X. Cao, W. Li, J. Wang, S. Wang, J. Memb. Sci. **495** (2015) 130.
[2] V. Gitis, G. Rothenberg, *Ceramic membranes: new opportunities and practical applications*, Wiley-VCH, Weinheim (2016).
[3] M. Mulder, *Basic principles of membrane technology*, Springer, Dordrecht (1990).
[4] A.K. Pabby, S.S.H. Rizvi, A.M. Sastre, *Handbook of membrane separations: chemical, pharmaceutical, food, and biotechnological applications*, 2nd ed., CRC Press

(2015).
[5] K. Li, *Ceramic membranes for separation and reaction*, Wiley, London (2007).
[6] R. Sondhi, R. Bhave, G. Jung, Membr. Technol. **2003** (2003) 5.
[7] B. Achiou, H. Elomari, A. Bouazizi, A. Karim, M. Ouammou, A. Albizane, J. Bennazha, S.A. Younssi, I.E. El Amrani, Desalination **419** (2017) 181.
[8] E. Garmsiri, Y. Rasouli, M. Abbasi, A.A. Izadpanah, J. Water Process. Eng. **19** (2017) 81.
[9] A. Oun, N. Tahri, S. Mahouche-Chergui, B. Carbonnier, S. Majumdar, S. Sarkar, G.C. Sahoo, R. Ben Amar, Sep. Purif. Technol. **188** (2017) 126.
[10] R.V. Kumar, A.K. Ghoshal, G. Pugazhenthi, J. Memb. Sci. **490** (2015) 92.
[11] H. Bissett, J. Zah, H.M. Krieg, Powder Technol. **181** (2008) 57.
[12] J. Caro, Chem. Soc. Rev. **45** (2016) 3468.
[13] P. Maarten Biesheuvel, A. Nijmeijer, H. Verweij, AIChE J. **44** (1998) 1914.
[14] N. Benes, A. Nijmeijer, H. Verweij, in: Recent Adv. Gas Sep. Micropor. Ceram. Membr., N.K. Kanellopoulos (Ed.), Elsevier (2000) 335.
[15] A. Nijmeijer, C. Huiskes, N.G.M. Sibelt, H. Kruidhof, H. Verweij, Am. Ceram. Soc. Bull. **77** (1998) 95.
[16] G.C. Steenkamp, H.W.J.P. Neomagus, H.M. Krieg, K. Keizer, Sep. Purif. Technol. **25** (2001) 407.
[17] P. Wang, P. Huang, N. Xu, J. Shi, Y.S. Lin, J. Memb. Sci. **155** (1999) 309.
[18] K. Guan, W. Qin, Y. Liu, X. Yin, C. Peng, M. Lv, Q. Sun, J. Wu, J. Memb. Sci. **520** (2016) 166.
[19] R.P.S. Dutra, L.R. de A. Pontes, Cerâmica **48** (2002) 223.
[20] H.J. Alves, F.G. Melchiades, A.O. Boschi, Cerâm. Ind. **18** (2013) 35.
[21] C.H. Chen, K. Takita, S. Ishiguro, S. Honda, H. Awaji, J. Eur. Ceram. Soc. **25** (2005) 3257.
[22] J.A. Queiroga, D.F. Souza, E.H.M. Nunes, A.F.R. Silva, M.C.S. Amaral, V.S.T. Ciminelli, W.L. Vasconcelos, Sep. Purif. Technol. **190** (2018) 195.
[23] C.A. Contreras, S. Sugita, E. Ramos, L.M. Torres, J. Serrato, AZo J. Mater. **2** (2006) 1.
[24] M.M. Martín-Ruiz, L.A. Pérez-Maqueda, T. Cordero, V. Balek, J. Subrt, N. Murafa, J. Pascual-Cosp, Ceram. Int. **35** (2009) 2111.
[25] R.E.P. Salem, A.S.A. Chinelatto, A.L. Chinelatto, Cerâmica **60** (2014) 108.
[26] K.H. Kim, S.J. Cho, K.J. Yoon, J.J. Kim, J. Ha, D.I.I. Chun, J. Memb. Sci. **199** (2002) 69.
[27] P.M. Biesheuvel, V. Breedveld, A.P. Higler, H. Verweij, Chem. Eng. Sci. **56** (2001) 3517.
[28] X. Sui, X. Huang, Sep. Purif. Technol. **32** (2003) 73.
[29] P. Monash, G. Pugazhenthi, P. Saravanan, Rev. Chem. Eng. **29** (2013) 357.
[30] A. Harabi, F. Bouzerara, S. Condom, Desalin. Water Treat. **6** (2009) 222.
[31] L.C. Dejonghe, M.N. Rahaman, in: Handb. Adv. Ceram. Mater. Appl. Process. Prop. (2007) 187.
[32] V.A. Patterson, H.M. Krieg, R.J. Kriek, H. Bisset, J. Memb. Sci. **285** (2006) 1.
[33] W. Zhang, M. Gaggl, G.J.G. Gluth, F. Behrendt, J. Environ. Sci. **26** (2014) 140.
[34] R.J.R. Uhlhorn, K. Keizer, A.J. Burggraaf, J. Memb. Sci. **46** (1989) 225.
(Rec. 10/09/2018, Rev. 10/11/2018, Ac. 03/12/2018)